J. Membrane Biol. 113, 115–122 (1990)

The Journal of
Membrane Biology
© Springer-Verlag New York Inc. 1990

Nonselective Cation Channel Activated by Patch Excision from Lobster Olfactory Receptor Neurons

Timothy S. McClintock* and Barry W. Ache
The Whitney Laboratory and Departments of Zoology and Neuroscience, University of Florida, St. Augustine, Florida 32086

Summary. A nonselective cation channel activated by patch excision was characterized in inside-out patches from spiny lobster olfactory receptor neurons. The channel, which was permeable to Na^+, K^+ and Cs^+, had a conductance of 320 pS and was weakly voltage dependent in the presence of micromolar divalent cations. Millimolar internal divalent cations caused a voltage- and concentration-dependent block of Na^+ permeation. Analysis of the voltage dependence indicated that the proportion of the membrane's electric field sensed by Mg^{2+} was > 1, suggesting that the channel contains a multi-ion pore. Internal divalent cations also reduced the frequency of channel opening in a concentration-dependent, but not voltage-dependent, manner, indicating that different cation binding sites affect gating and conductance. While block of gating prevented determining if internal divalent cations permeate the channel, a channel highly permeable to external divalent cations was observed upon patch excision to the inside-out configuration. The monovalent and divalent cation conductances shared activation by patch excision, weak voltage dependence, and steady-state activity, suggesting that they are the same channel. These data extend our understanding of this type of channel by demonstrating permeation by monovalent cations, detailing Mg^{2+} block of Na^+ permeation, and demonstrating the channel's presence in arthropods.

Key Words ion channels · channel blockers · olfaction · sensory cells · lobster

Introduction

Nonselective cation channels are diverse and encompass several functionally distinct subgroups. Best known are Ca^{2+}-activated nonselective cation channels (Partridge & Swandulla, 1988) and ligand-gated nonselective cation channels such as the acetylcholine receptor and the *c*GMP-gated channel of photoreceptors. A third and smaller group consists of nonselective cation channels activated by patch excision. These channels have previously been described only in molluscan neurons (Chesnoy-Marchais, 1985; Strong et al., 1987; Yazejian & Byerly, 1989). They have a relatively high conductance for divalent cations, are voltage independent or only weakly voltage dependent, and have conductances and kinetic properties dependent upon the types and quantities of permeant cations present. Patch excision activates these channels by mechanisms which remain unknown, though Ca^{2+} and ATP may play a role (Yazejian & Byerly, 1989; Strong et al., 1987).

We now describe a nonselective cation channel activated by patch excision from spiny lobster olfactory receptor neurons. We demonstrate that monovalent cations permeate the channel and show that internal divalent cations, especially Mg^{2+}, cause two types of block, a voltage-dependent decrease in the single channel conductance and a voltage-independent decrease in the frequency of channel opening. Analysis of the voltage-dependence of block suggests the channel has a multi-ion pore. The difference in voltage dependence between the two types of block suggests that separate cation binding sites mediate each type of block.

Materials and Methods

Preparation of Receptor Cells

Specimens of the spiny lobster, *Panulirus argus*, were collected in the Florida Keys and maintained in running seawater for up to three months. One of the paired olfactory organs (lateral filament of the antennule) was excised and cut into 0.5 mm long hemicylinders as described by Anderson and Ache (1985) in order to expose the clusters of olfactory receptor cell somata which fill the ventral one half of the lumen of the filament. The hemicylinders were gently agitated with papain activated by L-cysteine (0.25 mg/ml; Sigma, type IV) for 20 min and then with trypsin (2.5–5 mg/ml; Sigma, type IX) for an additional 20 min. Hemi-

* *Present address:* Section of Molecular Neurobiology, Yale University School of Medicine, 333 Cedar St., New Haven, CT 06510.

Table. Composition of solutions used in mM

	Saline	Low divalent saline	Ca^{2+} saline	Ba^{2+} saline	NaCl saline	Na^+ patch
NaCl	460	480	420	420	480	190
KCl	13	13				
$CaCl_2$	13	0.01	60		0.01	1
$MgCl_2$	10					
$BaCl_2$				60		
EGTA						11
HEPES-NaOH	10	20	10	10	20	20
Glucose		1.7			1.7	598
NaOAc						130

cylinders, or somata isolated from them by trituration with a glass pipette, were placed in a 35-mm culture dish for patch-clamp recording. Cells were viewed at 200× or 300× under brightfield or modulation contrast optics.

Patch-Clamp Recording

Gigaohm seals were made with borosilicate glass pipettes (H15/10/0181, Jencons Scientific, Leighton Buzzard, England) pulled and fire-polished to tip diameters of less than 1 μm, (bubble numbers of 3 to 4; Mittman et al., 1987). Single channel currents were amplified with a patch-clamp amplifier and a 10 GΩ head stage (Dagan, Minneapolis, MN). Records were filtered at 10 kHz for storage on videotape (Bezanilla, 1985) and at 0.5 to 5 kHz for analysis, using an eight pole low-pass Bessel filter (Frequency Devices, Haverhill, MA). An IBM XT microcomputer with an A/D, D/A converter and accompanying software (pClamp, Axon Instruments, Burlingame, CA) was used both to apply voltage step protocols and to digitize and analyze single channel records. Kinetic analysis was performed only on records from patches containing one active channel. Open and closed duration distributions were compiled as histograms and exponential probability density functions were fitted to them by a chi-square minimization method. Voltages for cell-attached patches are reported as the voltage applied across the membrane, without reference to the contribution of the membrane potential of the cell (not measured), following the convention of the internal potential being negative with respect to the external potential. Mean values are reported ± 1 SD.

Solutions

The compositions of patch solutions and salines are listed in the Table. HEPES and EGTA were obtained from Research Organics (Cleveland, OH) and inorganic salts from Fisher Scientific (Fair Lawn, NJ). All other chemicals were obtained from Sigma (St. Louis, MO). Calcium concentrations in EGTA solutions were calculated according to Hagiwara (1983). Solutions were buffered to pH 7.4 with HEPES.

Solution changes were made by moving inside-out patches through a slot cut into two concentric Delrin rings, one of which was fixed in the bath. The outer ring was then turned about the fixed inner ring to isolate a 300-μl chamber from the remainder of the bath. A push-pull syringe system allowed changing the solution in the chamber independently of that in the remainder of the bath. Alternatively, the patch was moved into a flow from a glass pipette (100 μm tip diameter) connected by a switching valve to six solution reservoirs.

Results

Conductance and Effects of Monovalent Ions

The nonselective cation channel was frequently observed in inside-out patches excised from receptor cell somata bathed in low divalent saline, but was never clearly observed in cell-attached patches. This channel had a linear current-voltage relationship with low divalent saline in the bath and Na^+ patch solution in the pipette (Fig. 1*A*,*B*). The mean slope conductance was 320 ± 21 pS (N = 19). Replacing Na^+ with K^+ in the patch pipette or with Cs^+ in the bath caused the reversal potential to shift to values intermediate between the Nernst potentials of Na^+ and K^+ or Cs^+, respectively. Permeability ratios for K^+ relative to Na^+ were 0.66 and 0.74 for two channels tested, and for Cs^+ relative to Na^+ were 0.33 and 0.35 for two other channels. Substituting glutamate or gluconate for Cl^- in the bath (N = 3) failed to shift the reversal potential.

Replacing the 480 mM Na^+ in the intracellular solution with Cs^+ or K^+ caused a gradual reduction in the frequency of channel openings and total lack of activity within a few minutes. Reducing the Na^+ concentration to 20, 50, 100, or 200 mM by K^+ or Cs^+ substitution caused the same effect. Switching back to 480 mM Na^+ caused recovery of channel activity in only three of eight patches. The temporal correlation between these solution changes and changes in channel activity was poor, suggesting that the effect was not a simple Na^+ activation of gating.

Single Channel Kinetics

Subsequent measurements of the channel's properties were performed on inside-out patches with an intracellular solution containing 460 or 480 mM Na^+. With high intracellular Na^+, the cation channel rarely became inactive, even in patches which lasted longer than 1 hr. The probability of being in the open state (P_o) was increased by depolarization (Fig. 2*A*). Voltage dependence was analyzed by fitting these data to a linearized form of the Boltzmann equation (Fig 2*B*). Apparent gating charges, calculated from the slopes of these lines, had a mean value of 1.11 ± 0.06 equivalent charges (N = 5). The average half-maximal activation voltage was −37 ± 7 mV. Analysis of dwell times showed that

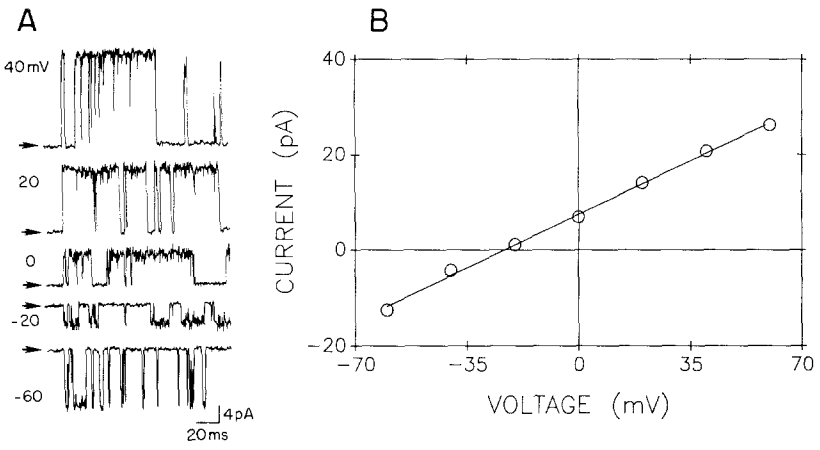

Fig. 1. A nonselective cation channel in an inside-out patch bathed in Na^+ patch solution and low divalent saline. (*A*) Representative records of the channel under conditions where Na^+ was the major charge carrier. Arrows indicate the current level of the closed state. Corner frequency (f_c) = 2 kHz. (*B*) A plot of the current-voltage relationship of the channel depicted in *A*. The slope conductance was 323 pS

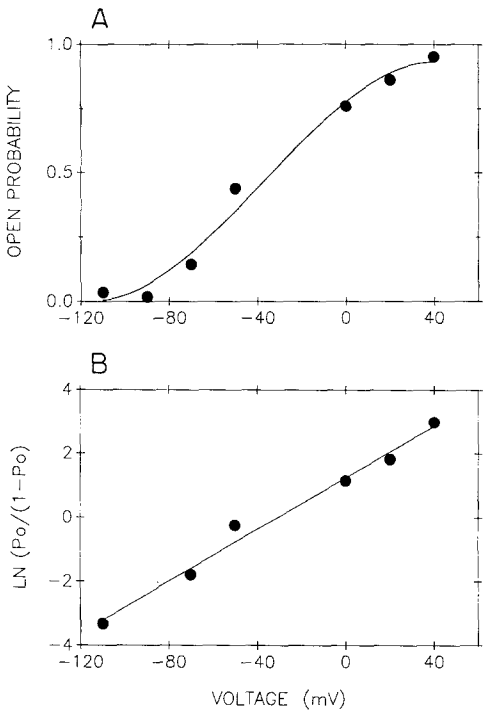

Fig. 2. The voltage dependency of the probability of the nonselective cation channel being in the open state (P_o). (*A*) Plot of the relationship of P_o and voltage for one channel. The curve was fitted to the data (points) by nonlinear regression. (*B*) Plot of the Boltzmann linearization of the data from *A*. The line was fitted to the data by linear regression

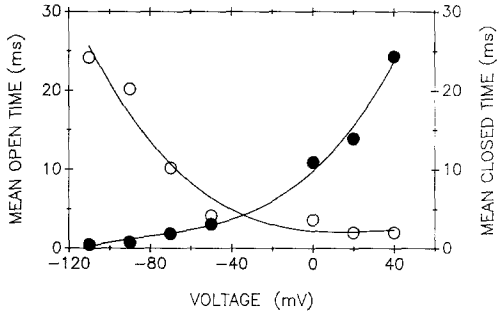

Fig. 3. Plot of voltage dependence of the mean open (filled circles) and closed times (open circles) of a nonselective cation channel. Depolarization increased the P_o by increasing the mean open time and decreasing the mean closed time. The curves were fitted to the data by nonlinear regression

the increase in P_o caused by depolarization was due to both increased mean open times and decreased mean closed times (Fig. 3). Most open dwell time distributions were fit best by a single exponential function, whereas closed dwell time distributions usually were better fit by a double exponential.

None of the properties of the cation channel were affected by perfusing the intracellular side of the patch with salines containing 10^{-10} to 10^{-4} M Ca^{2+}, nor were they affected by 10 μM *c*GMP (N = 10) or 10 μM *c*AMP (N = 8) applied to the same side. External tetrodotoxin (N = 1) and mouth suction or pressure applied to the pipette also had no discernible effect. A potent odor mixture (a filtered, saline extract of TetraMarin, TetraWerke, Melle, FRG) applied in the patch pipette failed to cause the appearance of this channel (or any other channel) in cell-attached patches or to alter the properties of the cation channel in inside-out patches (N = 33).

Block by Tetraethylammonium and Divalent Cations

Perfusion of the intracellular side of the channel with salines containing 20 or 50 mM tetraethylammonium chloride (TEA) caused a voltage-dependent channel block characterized by rapid flickering between the open and closed current levels (*data not shown*). Block by TEA was not pursued further. Block by internal divalent cations, however, provided clues about the pore morphology and kinetic

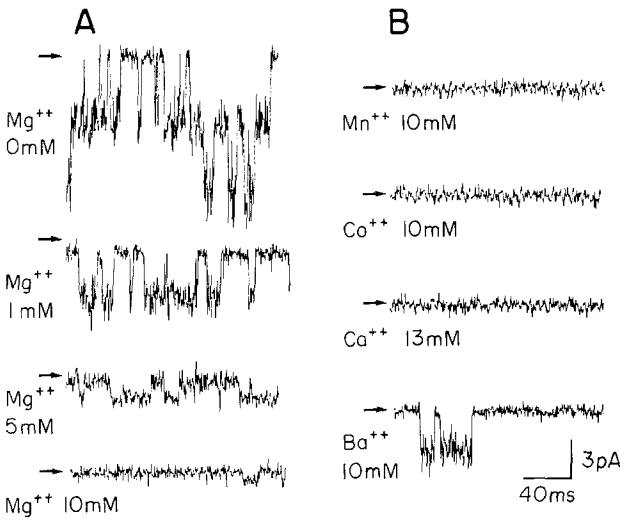

Fig. 4. Representative records showing the blocking effect of divalent cations applied to the intracellular side of inside-out patches containing a nonselective cation channel. (*A*) The concentration dependence of block by Mg^{2+}. All records obtained from the same patch containing three cation channels. (*B*) 10 mM or more Mn^{2+}, Co^{2+}, and Ca^{2+} appeared to reduce the open channel amplitude below the limit of resolution. 10 mM Ba^{2+} blocked the channel much less effectively than the other ions. These records were from several different patches containing a single cation channel. All records were obtained at −25 mV in symmetrical 480 mM NaCl and low pass filtered at a corner frequency of 1.5 kHz. Arrows indicate the current level of the closed state

properties of this channel. Ba^{2+}, Ca^{2+}, Mn^{2+}, Co^{2+}, and Mg^{2+}, at concentrations from 1 to 13 mM, all reduced the open channel amplitude in a manner characteristic of very fast blocking kinetics (Fig. 4*A,B*). The block by Mg^{2+}, the only divalent cation likely to occur at millimolar intracellular concentrations, was investigated in detail.

In fast block, Mg^{2+} decreased the apparent open channel amplitude in a concentration-dependent manner (Fig. 4*A*). The dissociation constant of Mg^{2+} for the binding site, or sites, responsible for fast block was obtained by analyzing the blocker titration curve of Mg^{2+} (Fig. 5*A*) in which the ratio of the blocked to the unblocked channel amplitude (i_B/i) is the fraction of time a channel is not occupied by the blocker (Moczydlowski, 1986). At binding equilibrium between n blocker molecules and the open channel (Eq. (1)), the equations describing the blocker titration curve (Eq. (2)) and its Hill plot (Eq. (3)) are

$$nB + O \overset{K_B}{\longleftrightarrow} nB \cdot O \tag{1}$$

$$i_B/i = (1 + [B]^n/K_B^n)^{-1} \tag{2}$$

$$\ln(i/i_B - 1) = n \cdot \ln[B] - n \cdot \ln K_B \tag{3}$$

where $[B]$ is the concentration of blocker, n is the Hill coefficient, and K_B is the dissociation constant of the blocker. The Hill coefficient (n) and dissociation constant (K_B) obtained from data pooled from two patches exposed to 1 to 10 mM Mg^{2+} were 1.07 and 1.6 mM, respectively (Fig. 5*B*).

Fast block by Mg^{2+} was also voltage dependent, reaching a maximum between −30 and −10 mV (Fig. 5*C*), possibly corresponding to the Na^+ reversal potential (E_{Na}) of −23 mV. This observation suggested that Mg^{2+} interacted with Na^+ in the permeation pathway and that Mg^{2+} might even be slightly permeable. The voltage dependence of the fast block was analyzed according to the Woodhull (1973) model, which assumes that voltage dependence arises because the binding site for a charged blocking particle lies within the membrane's electric field, such as in the channel pore. The data from membrane potentials below E_{Na} were linearized and estimates of K_B and of $z\delta$, the proportion of the membrane's electric field sensed by a charged blocking particle at its binding site, were obtained from the following equation (Moczydlowski, Uehara & Hall, 1986):

$$\ln[(i/i_B) - 1] = z\delta FV/RT + \ln([B]/K_B) \tag{4}$$

where n is assumed to be 1. Estimates of K_B averaged 39 ± 16 μM Mg^{2+} (N = 5). Estimates of $z\delta$ averaged 2.6 ± 0.2 (N = 5), indicative of multiple blocker binding sites. These values were then used to calculate the expected current-voltage relationship in the presence of 3 mM Mg^{2+}. Comparison of the calculated curve with actual data (Fig. 5*D*) further demonstrates the voltage-dependent relief of block suggestive of Mg^{2+} permeability.

In addition to fast block, Mg^{2+} also caused a voltage-independent reduction in the frequency of openings, which is apparent in the concentration-dependent decrease in channel activity in Fig. 4*A*. The difference in voltage dependency between this slow block and fast block suggests that distinct binding sites, or sets of binding sites, mediate the two types of block. For any given channel, slow block was dependent upon the concentration of Mg^{2+}, but the magnitude of the reduction in P_o varied between channels (*data not shown*). Slow block was not limited to Mg^{2+}, as 10 mM Ba^{2+} applied internally reduced the P_o of one channel from 0.84 to 0.25 at −20 mV.

Permeability to Ca^{2+} and Ba^{2+}

The finding that holding potentials more positive than E_{Na} relieved the block by Mg^{2+} raised the possibility that divalent cations could permeate this

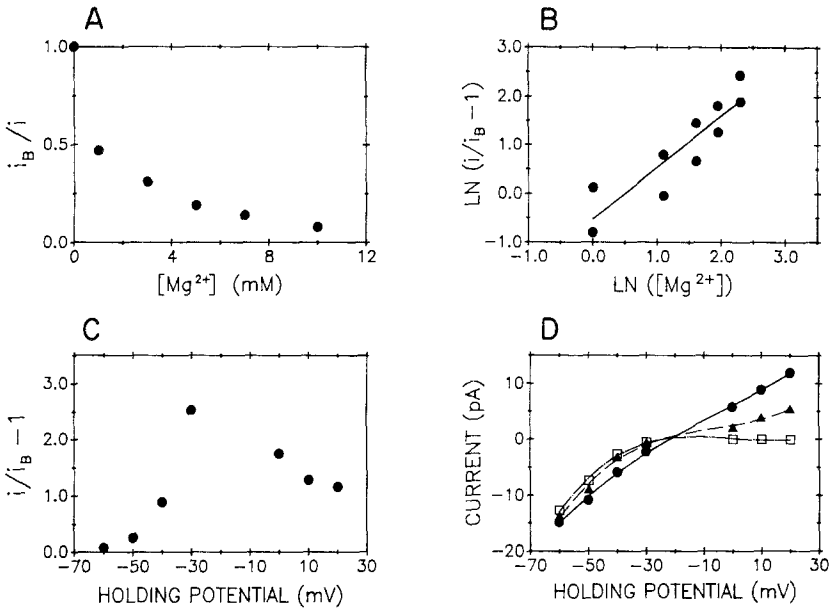

Fig. 5. Analysis of the Mg^{2+} block of the nonselective cation channel. (*A*) A representative plot of the blocker titration curve from one patch; the blocked single channel current normalized to the unblocked current as a function of the concentration of Mg^{2+} at 0 mV. (*B*) Plot of the fit of the Hill equation to data pooled from two patches titrated with Mg^{2+}. A linear regression of these data yielded a Hill coefficient of 1.07 and a dissociation constant of 1.6 mM. (*C*) Plot of the voltage dependence of block of 3 mM Mg^{2+} for one patch; block is relieved to differing extents by hyperpolarization and depolarization. (*D*) A plot of the current-voltage relationship in the absence (circles, solid line) and presence (triangles, dashed line) of intracellular Mg^{2+} at 3 mM. The expected current voltage relationship in the presence of 3 mM Mg^{2+} (squares, dot-dashed line) calculated from the voltage dependence of block below E_{Na} (−23 mV) demonstrates the relief of block above E_{Na}. Lines were fitted to the data by nonlinear regression

channel. To test this possibility, the internal faces of inside-out patches containing cation channels were perfused with 60 mM divalent cations. This manipulation, however, eliminated all channel activity, possibly due to the slow block by divalent cations described above. Because stable outside-out patches were difficult to obtain in low divalent saline (K. Schütte and T.S. McClintock, *unpublished observations*), channel activity presumably corresponding to the cation channel was subsequently recorded in inside-out patches from cells bathed in low divalent saline when either Ca^{2+} or Ba^{2+} saline was in the patch pipette. Under these conditions, unitary inward currents were observed at potentials above E_{Na} (−3 mV) and E_{Cl} (−11 mV) where they could only be carried by the divalent cation (Fig. 6*A,B*). The properties of these divalent permeable channels—no inactivation, weak voltage dependence, and activity in inside-out, but not cell-attached, patches—correlate with those of the nonselective cation channel. The slope conductance of the channel in Ba^{2+} saline was 80 pS (measured by regression of data from −70 to −30 mV), while values of 43 and 44 pS (by regression from −110 to −60 mV) were measured in Ca^{2+} saline (Fig. 6*C*). If these channels were the same cation channel found in solutions with low divalent cation concentrations, the P_o in Ba^{2+} saline was much reduced (e.g., $P_o = 0.39$ at −5 mV versus > 0.75, *cf.* Fig. 2). The effect of Ca^{2+} saline was even more dramatic in that the P_o increased to 0.1 at −10 mV, but failed to increase further with stronger depolarization.

A Cell-Attached Cation Conductance

The nonselective cation channel was never clearly apparent in cell-attached patches, even in those that demonstrated cation channel activity after excision to the inside-out configuration. With NaCl or KCl solutions containing micromolar divalent cations in the patch pipette, however, large inward current events whose kinetics were too rapid to permit accurate measurement of the current amplitude occurred in cell-attached patches on cells bathed in low divalent saline (Fig. 7). This channel activity was not observed with millimolar concentrations of divalent cations in the pipette, and only rarely occurred in cells bathed in salines containing millimolar concentrations of divalent cations. Depolarization decreased the apparent amplitude and increased the frequency of these current transients. This type of channel activity did not inactivate, even at applied potentials of 60 mV or more, arguing against the interpretation that this activity was

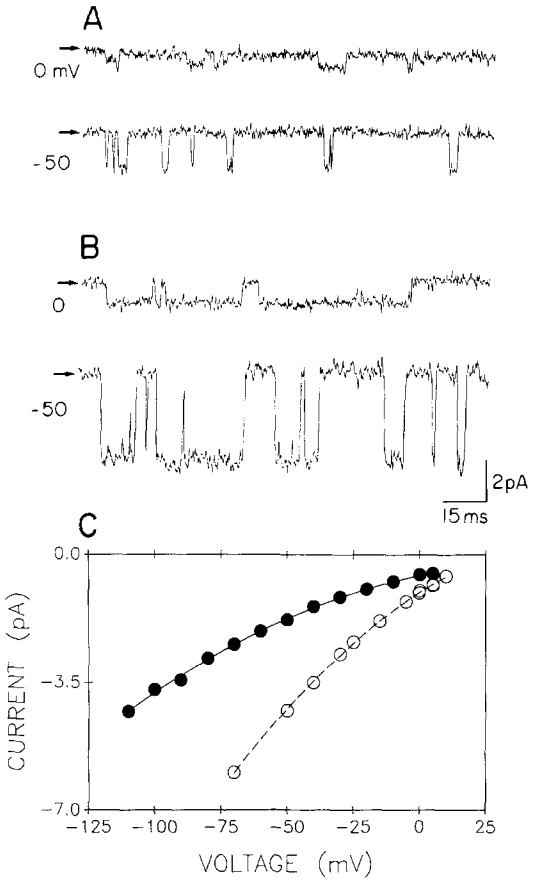

Fig. 6. Inward current events carried primarily by Ba^{2+} and Ca^{2+} through putative nonselective cation channels in inside-out patches. (*A*) Representative records showing inward current events in Ca^{2+} saline. The patch contained two channels, indicated by simultaneous open events summing to twice the single channel current amplitude (*not shown*). Arrows indicate the current level of the closed state. f_c = 1 kHz. (*B*) Representative records showing inward current events in Ba^{2+} saline. The patch contained three channels. f_c = 1 kHz. (*C*) Plot of the current-voltage relationships of the data represented in *A* and *B* in external Ca^{2+} saline (filled circles) and in Ba^{2+} saline (open circles). Note the inward rectification. Curves were fitted to the data by nonlinear regression

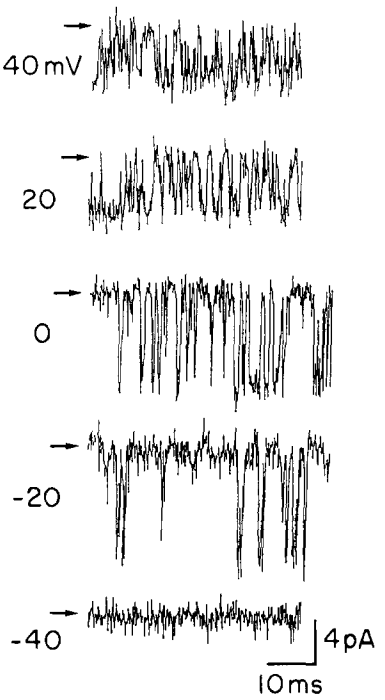

Fig. 7. Representative records of a putative nonselective cation channel in a cell-attached patch. Note the rapid transitions between the open and closed states of the channel. This was the record with the slowest kinetics observed. The pipette contained NaCl saline. Arrows indicate the current level of the closed state. f_c = 2 kHz

Na^+ flowing through Ca^{2+} channels in the absence of external divalent cations (Almers, McCleskey & Palade, 1984). When excised into the inside-out configuration, 65% of these patches contained one or more of the nonselective cation channels described above, but no other channel activity. Less than 40% of the silent cell-attached patches showed cation channel activity after being excised. Contingency table analysis of these proportions showed a significant interaction of cell-attached and inside-out cation channel activity (chi square = 4.1, $P < 0.05$, 1 *df*, $N = 119$). These observations allow that the two types of kinetic activity could correspond to a single species of cation channel experiencing different biochemical environments imposed by cell-attached and inside-out recording configurations.

Discussion

The nonselective cation channel we describe shares several properties with a type of channel described in molluscan neurons (Chesnoy-Marchais, 1985). (i) It is resolved only in excised patches. (ii) High internal concentrations of Na^+, but not Cs^+ or K^+, appear to prevent inactivation of the channel. (iii) Its kinetics are sensitive to the type of divalent cation present. (iv) It is weakly voltage dependent. (v) Its activity is reduced by internal Ca^{2+} and Ba^{2+}. (vi) It appears to have a multi-ion pore. If the channel in lobster olfactory receptor cells is permeable to divalent cations, as our data suggest, then additional shared properties are that (vii) Ba^{2+} gives a higher conductance than Ca^{2+} and (viii) the current-voltage relationship of the channel shows inward rectification in high external concentrations of divalent cations, especially at potentials above E_{Na}. These similarities indicate that this type of channel is not unique to molluscan neurons and is therefore

more likely to be of general significance for neuronal function.

Our demonstration of Na^+ permeability confirms recordings of macroscopic currents, which suggested that Na^+ could permeate this type of channel (Yazejian & Byerly, 1989). We show that K^+ and Cs^+ are also permeable, although less so than Na^+. The permeability of monovalent cations provides an explanation for the rectification in *I-V* relationships when current is carried by divalent cations. Monovalent cations could act as weak blocking ions whose efficacy would depend on the driving forces upon the monovalent cations relative to those upon the divalent cations. Not surprisingly, rectification becomes greater closer to the Nernst potential for the divalent cations.

Our finding that Mg^{2+} blocks Na^+ permeation in this type of channel is novel and offers a partial glimpse of the structure of the channel. The channel may contain multiple cation binding sites within its pore because block by Mg^{2+} had a voltage dependence described by apparent electrical distances > 1. The channel also appears to have another divalent cation binding site outside the electric field of the membrane capable of altering the gating properties of the channel because the reduction in P_o caused by Mg^{2+} had little voltage dependence. This latter site may be very near the permeation pathway, however, since both internal and external permeable divalent cations decreased the P_o. Alternatively, another, external binding site could exist. The existence of separate cation binding sites affecting conductance and gating was previously postulated by Chesnoy-Marchais (1985) based on differences in the relative sequences of divalent cation conductance and ability to alter gating in what appears to be a similar channel from molluscan neurons.

In addition to agreeing with the Woodhull model of channel block (Woodhull, 1973), the interpretation that fast block is due to Mg^{2+} entering the channel's pore is consistent with evidence that Na^+ and Mg^{2+} compete for binding sites, namely that the dissociation constant for Mg^{2+} depended on the direction of flow of Na^+ through the pore. When the holding potential was above E_{Na} at 0 mV, where Na^+ should force internal Mg^{2+} through the pore, the apparent dissociation constant was in the millimolar range. When the holding potential was below E_{Na}, where Na^+ should oppose the permeation of internal Mg^{2+} through the pore, the apparent dissociation constant was 40-fold less. These differences in the interaction of Na^+ and Mg^{2+} within the pore may also account for the absence of evidence for multiple binding sites given by the concentration dependence of Mg^{2+} block (n = 1.07), since this measurement was made at 0 mV. Larger Hill coefficients might be measured at other membrane potentials, especially at potentials below E_{Na}. Further confirmation of a multi-ion pore could be obtained by determining if Na^+ causes an increase in the dissociation rate constant of Mg^{2+} (Moczydlowski, 1986).

If the channels that were permeable to divalent cations are, in fact, the nonselective cation channel, then the divalent cations replaced Na^+ as the major permeant ion. Ca^{2+} or Ba^{2+} can supersede monovalent cations as major permeant ions in channels when they bind more strongly to sites within the channel pore, effectively excluding the monovalent cation (Almers et al., 1984; Dani & Eisenman, 1987). A necessary corollary of this assertion is that Ca^{2+} and Ba^{2+} should have lower conductances than Na^+. While our data do not directly address this point, Ba^{2+}, which appeared to bind less strongly within the pore than Ca^{2+} by virtue of its weaker blocking ability, gave a higher conductance than Ca^{2+} under identical conditions. Furthermore, the properties of the fast block by Mg^{2+} strongly suggest that divalent cations bound more strongly to sites within the pore than monovalent cations.

Our data further indicate that internal divalent cations reduced the P_o by interacting with sites apparently outside the electric field of the membrane. The effect appeared to be mediated by a site (or sites) on the channel protein and not by charge screening of the diffuse negative charges on the membrane (which alters the surface potential and effectively changes the profile of potential across the membrane). Charge screening by internal cations should cause a negative shift in the activation curve of voltage-dependent channels (McLaughlin, Szabo & Eisenman, 1971), whereas we observed a positive shift.

The function of this type of nonselective cation channel will probably remain a mystery until the discovery of the mechanism of activation of the channel. The channel appears to be activated, or released from inactivation, by the change in internal environment caused by patch excision rather than mechanical stress because the application of positive and negative pressure to the pipette, the definitive criteria for stretch-activated channels (Kullberg, 1987), failed to affect the channel. The possibility that the channel has an undetectably small conductance in physiological solutions due to Mg^{2+} block or a mole fraction effect is unlikely. If the physiological conductance was simply small, the channel should have been detectable in cell-attached patches when low divalent saline or Ca^{2+} or Ba^{2+} saline was in the patch pipette. Alternatively, the channel may be normally inactive, perhaps due

to slow block by Mg^{2+}, and only function in physiologically stressful conditions. High internal Na^+ concentrations, as might occur in injured cells, were important in maintaining the channel activity, which might explain the lack of channel activity in cell-attached patches. Our data, however, indicate that activation of this channel is more complex than a simple Na^+-dependent gating mechanism. Strong et al. (1987) only observed a similar channel in cell-attached patches from *Aplysia* neurons following injury to the cell's neurites. Yazejian and Byerly (1989) found that a similar channel in *Lymnaea stagnalis* neurons could be activated by sustained intracellular perfusion with high Ca^{2+} solutions or low Ca^{2+} solutions lacking ATP, or by a low Ca^{2+}, high K^+ bath solution. Since our data come from cells bathed in low divalent saline after being stripped of their neurites, it is possible that this species of cation channel is somehow involved in responses to trauma in the spiny lobster. Damage to neurites might be expected to occur naturally in neurons whose dendrites are directly exposed to the environment like those of olfactory receptor cells.

We thank Drs. P.A.V. Anderson and C. Miller for advice and for critically reading a draft of the manuscript. We thank J.D. Young for technical assistance and M.L. Milstead and J. Netherton for help with the figures. This work was supported by NIMH Fellowship F31MH09495 and NSF Award 85-11256.

References

Almers, W., McCleskey, E.W., Palade, P.T. 1984. A nonselective cation conductance in frog muscle membrane blocked by micromolar external calcium ions. *J. Physiol. (London)* **353:**565–583

Anderson, P.A.V., Ache, B.W. 1985. Voltage- and current-clamp recordings of the receptor potential in olfactory receptor cells in situ. *Brain Res.* **338:**273–280

Bezanilla, F. 1985. A high capacity recording device based on a digital audio processor and a video cassette recorder. *Biophys. J.* **47:**437–441

Chesnoy-Marchais, D. 1985. Kinetic properties and selectivity of calcium-permeable single channels in *Aplysia* neurons. *J. Physiol. (London)* **367:**457–488

Dani, J.A., Eisenman, G. 1987. Monovalent and divalent cation permeation in acetylcholine receptor channels. *J. Gen. Physiol.* **89:**959–983

Hagiwara, S. 1983. Membrane Potential-dependent Ion Channels in Cell Membrane. 118 pp. Raven Press, New York

Kullberg, R. 1987. Stretch-activated ion channels in bacteria and animal cell membranes. *Trends Neurosci.* **10:**387–388

McLaughlin, S.G.A., Szabo, G., Eisenman, G. 1971. Divalent ions and the surface potential of charged phospholipid membranes. *J. Gen. Physiol.* **58:**667–687

Mittman, S., Flaming, D.G., Copenhagen, D.R., Belgum, J.H. 1987. Bubble pressure measurement of micropipet tip outer diameter. *J. Neurosci. Meth.* **22:**161–166

Moczydlowski, E. 1986. Single-channel enzymology. *In*: Ion Channel Reconstitution. C. Miller, editor. pp. 75–113. Plenum, New York

Moczydlowski, E., Uehara, A., Hall, S. 1986. Blocking pharmacology of batrachotoxin-activated sodium channels. *In*: Ion Channel Reconstitution. C. Miller, editor. pp. 405–428. Plenum, New York

Partridge, L.D., Swandulla, D. 1988. Calcium-activated nonspecific cation channels. *Trends Neurosci.* **11:**69–72

Strong, J., Fox, A.P., Tsien, R.W., Kaczmarek, L.K. 1987. Formation of cell-free patches unmasks a large, divalent-permeable, voltage-independent channel in *Aplysia* neurons. *Soc. Neurosci. Abstr.* **13:**1011

Woodhull, A.M. 1973. Ionic blockage of sodium channels in nerve. *J. Gen. Physiol.* **61:**687–708

Yazejian, B., Byerly, L. 1989. Voltage-independent, barium-permeable channel activated in *Lymnaea* neurons by internal perfusion or patch excision. *J. Membrane Biol.* **107:**63–76

Received 30 April 1989; revised 13 September 1989